

# Doppler images of the pre-main sequence binary V824 Arae<sup>\*</sup>

A.P. Hatzes<sup>1</sup> and M. Kürster<sup>2</sup>

<sup>1</sup> McDonald Observatory, The University of Texas at Austin, Austin, TX 78712-1083, USA

<sup>2</sup> European Southern Observatory, Casilla 19001, Vitacura, Santiago 19, Chile

Received 28 September 1998 / Accepted 1 March 1999

**Abstract.** A time series of spectral observations are used to derive the spot distribution on both components of the active late-type binary system V824 Ara. Both stars show a spot distribution that is dominated by a polar spot whose center is displaced from the rotation axis of the star. This is similar to the spot distribution found on other young stars and may provide further support for the hypothesis that V824 Ara is a pre-main sequence binary. The Doppler images of both components appear to be mirror images of each other and this suggests that tidal forces may influence the spot distribution on these stars.

**Key words:** stars: binaries: spectroscopic – stars: imaging – stars: individual: V 824 Ara – stars: pre-main sequence – stars: starspots

## 1. Introduction

The active binary V824 Ara (=HD 155555) exhibits all the characteristics nominally attributed to the RS CVn class of stars. This system, which consists of G0 + K0 (presumed main sequence) stars, is chromospherically active showing photometric variations attributed to cool spots as well as X-ray emission (Walter et al. 1980). Unlike the RS CVn stars which are evolved giants, there is increasing evidence that V824 Ara is, in fact, a young pre-main sequence system. Pasquini et al. (1991) argued for a pre-main sequence status for this system based on a number of reasons. (1) The space velocity for this binary is typical for young stars; (2) a high lithium content indicating an age younger than the Pleiades, and (3) strong H $\alpha$  emission in the M Dwarf third component to V824 Ara that is characteristic of a young age. Martin & Brandner (1995) found that the M dwarf companion showed large lithium depletions. This was attributed to pre-main sequence lithium destruction which takes place on timescales of  $\sim 10^6$  yrs. They concluded that the evolutionary status of the system is intermediate between T Tauri stars and Pleiades low mass stars.

V824 Ara is an important system for two reasons. If it is indeed a pre-main sequence system then it represents an ac-

tive star system different from the RS CVn-type stars which are evolved giants. Doppler images have been derived for relatively few young stellar objects and most of these have been weak T Tauri stars. The Doppler images for V410 Tau (Strassmeier et al. 1994, Joncour et al. 1994, Hatzes 1995) and HDE 283572 (Joncour et al. 1995) were all characterized by a large decentered polar spot. On V410 Tau this feature was similar to one derived from photometric modelling using data from 1987 (Herbst 1989) and this suggests that this feature is stable and long-lived.

Fewer Doppler images have been derived for stars that have evolved past the T Tauri stage and have recently arrived on the main sequence. The best studied of these, AB Dor (K0V), shows both high and low latitude spot activity. In one epoch the spot distribution was dominated by a low-latitude band of activity (Kürster et al. 1994). At other times it showed both a high and low-latitude active band (Unruh et al., 1995) or a spot distribution dominated by features above latitude 60° (Donati & Collier Cameron 1997).

Stout-Batalha & Vogt (1996) presented images for two zero age main sequence stars in the Pleiades and these were characterized by both polar spot and low latitude band activity. Clearly, Doppler images of a larger sample of young stars, particularly those spanning a range of ages, are needed to understand the morphological differences between spots on these stars and the more evolved RS CVn-type stars as well as to discern changes in this morphology with stellar age.

A second important reason for Doppler imaging V824 Ara is that it is young *binary* system. Previous Doppler images of young objects have been for single stars. Tides may influence the spot distribution on active stars, but this can only be examined by imaging young stars in short-period binaries as well. Furthermore, both components of V824 Ara are rapidly rotating late-type stars and as such they both should be magnetically active. V824 Ara represents one of the few opportunities to compare the spot distribution on both components of a binary system.

## 2. Observations

Spectroscopic observations of V824 Ara were taken in September 1990 using the ESO 1.4-m coudé auxiliary telescope (CAT) equipped with the coudé echelle spectrometer (CES). An RCA

---

Send offprint requests to: Artie Hatzes

(artie@astro.as.utexas.edu)

\* Based on observations collected at the European Southern Observatory

**Table 1.** Spectroscopic Observations for 1990

JD 244	Exp (min)	SNR	Phase
8142.532	15	265	0.356
8142.543	15	250	0.362
8142.554	15	290	0.369
8142.565	15	260	0.375
8142.687	15	210	0.448
8143.523	15	200	0.945
8143.545	15	225	0.958
8143.556	15	185	0.965
8143.637	15	240	0.013
8143.648	15	225	0.019
8143.659	15	230	0.026
8143.670	15	280	0.033
8143.682	15	250	0.040
8143.693	15	230	0.046
8144.469	15	240	0.508
8144.480	15	270	0.514
8144.491	15	230	0.521
8144.502	15	270	0.527
8144.557	15	230	0.560
8144.568	15	250	0.567
8144.579	15	250	0.573
8144.590	15	250	0.580
8149.641	15	170	0.583
8149.645	15	170	0.586
8149.664	15	180	0.597
8149.675	15	250	0.603
8150.555	15	160	0.127
8150.566	15	210	0.133
8150.576	15	170	0.139
8150.587	15	190	0.146
8151.486	15	160	0.680
8151.497	15	140	0.687
8151.507	15	150	0.693
8151.518	15	90	0.699
8152.608	15	180	0.348
8152.619	15	180	0.354

CCD (1030 pixels of size  $15 \mu\text{m}$  in the dispersion direction) detector provided a wavelength coverage of about  $53 \text{ \AA}$  centered on  $6444 \text{ \AA}$ . The spectral resolution was  $0.13 \text{ \AA}$  ( $\lambda/\Delta\lambda=50,000$ ). Data reduction was performed using the MIDAS software package developed at ESO and involved the standard steps of bias subtraction, division by the spectrum of a continuum source (flatfield), cosmic ray removal, spectrum extraction, wavelength calibration, and continuum normalization.

Table 1 lists the Julian Day of the observations, exposure times, signal-to-noise ratio per resolution element ( $SNR$ ), and stellar rotation phase for the three observing epochs. Phases were calculated according to the ephemeris of Pasquini et al. (1991):

$$HJD = 2, 446, 998.4102 + 1.681652E \quad (1)$$

Phase 0.0 corresponds to quadrature with component A having its maximum radial velocity.

### 3. Doppler imaging

Doppler images were derived for both components of V824 Ara using maximum entropy reconstruction principles and the Ca I  $6439 \text{ \AA}$ . The details of the reconstruction technique can be found in Vogt, Penrod, & Hatzes (1987). Before deriving a Doppler image one needs to know the projected rotational velocity and inclination of the star (see below).

#### 3.1. Pre-imaging data preparation

##### 3.1.1. Stellar parameters

The  $v \sin i$  was determined by fitting a rotationally broadened synthetic line profile to the mean shape of the observed Ca I  $6439 \text{ \AA}$  line produced by averaging all observed phases. Averaging the spectra over a complete rotation cycle weakens the distortions thus resulting in a better representation of the rotationally broadened profile. The synthetic profile was computed by performing a disk integration on a star divided into  $120 \times 120$  cells. Local line profiles were generated at 20 limb angles (to include the effects of limb darkening) using the SME spectral synthesis package (Valenti & Piskunov 1996). A macroturbulent velocity of  $4 \text{ km s}^{-1}$  and a microturbulent of  $1.5 \text{ km s}^{-1}$  were used in the computation. This process yielded a  $v \sin i_A$  of  $35 \pm 1 \text{ km s}^{-1}$  for component A and  $v \sin i_B = 33 \pm 1 \text{ km s}^{-1}$ . These are consistent with the values of  $v \sin i_A = 37 \pm 3 \text{ km s}^{-1}$  and  $v \sin i_B = 29 \pm 5 \text{ km s}^{-1}$  found by Pasquini et al. (1991).

Pasquini et al. (1991) adopted a value of  $52.5^\circ \pm 2.5$  for the inclination of V824 Ara. A lack of eclipses confined the orbital inclination to less than  $68^\circ$ . Using evolutionary tracks they excluded  $i < 50^\circ$  since the retrieved masses implied an effective temperatures much higher than allowed by photometric measurements.

The stellar inclination was derived from the Doppler imaging reconstruction using the procedure outlined by Hatzes et al. (1989). They demonstrated that the misfit between data and predicted line profiles ( $\chi^2$ ) was minimized when the correct stellar inclination was used in the reconstruction process. The co-author used the same technique to determine the inclination of AB Dor (Kürster et al. 1994). Fig. 1 shows the  $\chi^2$  (normalized by the minimum value) from the Doppler imaging reconstruction as a function of the input stellar inclination for a series of nine reconstructions. The  $\chi^2$  is minimized at  $i \approx 45^\circ$ . An inclination of  $49^\circ$ , which is an average of the value determined here and the one adopted by Pasquini et al. (1991), was used for all reconstructions. We would like to stress that the final Doppler image is relatively insensitive to changes in the stellar inclination by about  $\pm 20^\circ$  (Vogt et al. 1987; Kürster 1993).

The improved measurements of the  $v \sin i$  as well as the assumed inclination allows us to estimate the stellar radii of the components. Assuming that the orbital and rotation periods are identical one finds radii of  $R_A = 1.53 R_\odot$  and  $R_B = 1.44 R_\odot$  for the primary and secondary respectively. These are much larger than typical values for main sequence G0 and K0 stars. Clearly V824 Ara is not a main sequence binary system. For instance the K0V star AB Dor has a radius of  $\approx 1.1 M_\odot$  as shown in

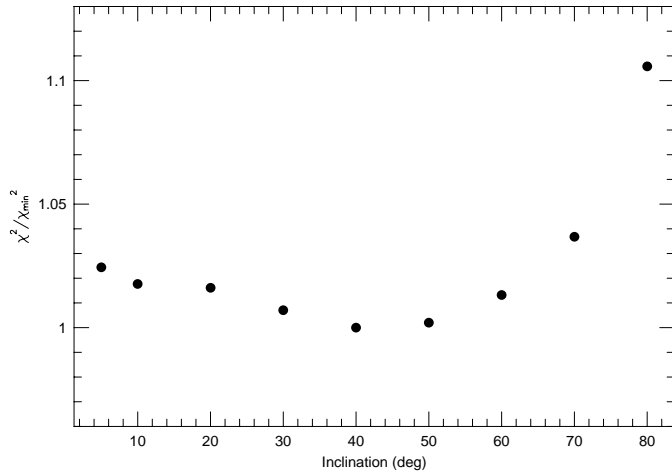


**Fig. 1.** The normalized  $\chi^2$  as a function of inclination used in the reconstruction

Kürster et al. (1994), so V824 Ara appears to be younger than AB Dor.

### 3.1.2. Deblending of stellar line profiles

As a final step in preparing the stellar spectra for Doppler imaging it was necessary to remove the contribution of the stellar profile of one component from the spectral line of the other component (i.e. deblend). This was done in the following manner. First, a synthetic, rotationally-broadened spectral line for each star was generated by fitting an observation at a phase when the spectral lines of each component were well separated in radial velocity. This established the relative depth ( $D_{A,B}$ ) of each of the line profiles ( $D_B/D_A = 1.047 \pm 0.015$ ). For the blended phase the relative separation between the two synthetic profiles was varied until the residuals between the observed and combined synthetic profiles were minimized. Because the continuum level is slightly different for each observation (primarily due to noise, flat field errors, and choice of continuum) it was sometimes necessary to alter the relative depths of the two profiles from their nominal values, but this was never more than a few percent. Once a good match was made to the observed blended profiles the synthetic profile of one component was removed from the observed profile of the other component and vice versa.

### 3.2. Component A image

A Doppler image of the primary component (G0) of V824 Ara was derived using 12 rotation phases. (To improve the signal-to-noise of the data the original 36 observations were co-added to produce 12 spectral line profiles for use in the reconstruction process.) These profiles are shown as crosses in Fig. 2. The Doppler image is shown as a grayscale, flattened polar representation (as viewed from above the visible pole) in Fig. 3.. Latitude lines are drawn at equally spaced intervals down to a stellar latitude of  $-30^\circ$ .

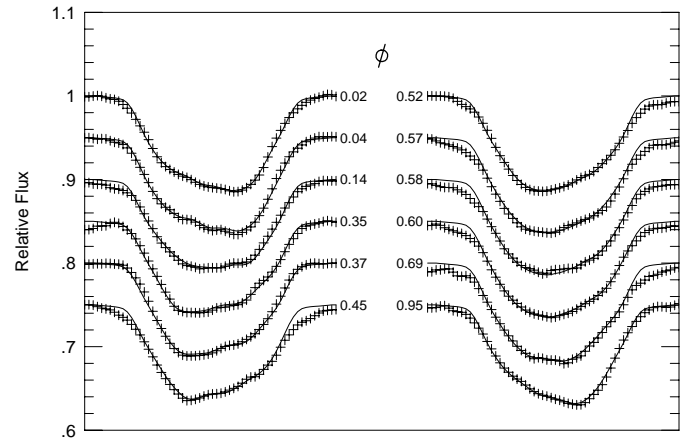


**Fig. 2.** The observed spectral line profiles of the Ca I 6439 Å line for V824 Ara A (crosses) and the fits from the Doppler image in Fig. 3

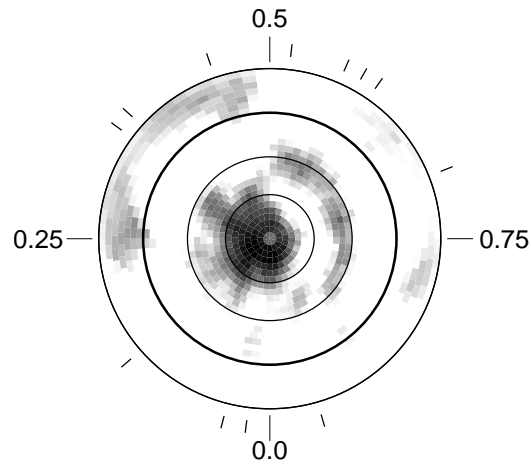


**Fig. 3.** Doppler image of V824 Ara A

The image is dominated by a large polar cap whose center is clearly displaced from the rotation pole of the star. There is also a band, or series of small spots situated at latitude  $+30^\circ$  between phases 0.50 and 0.88. The fits to the observed spectral line profile provided by the Doppler image are shown as lines in Fig. 2. A version of the image of V824 Ara A based on the same data set and produced with the CLEAN-like algorithm was shown in the Kürster et al. (1992). This image is consistent with the maximum entropy version presented here.

### 3.3. Component B image

The Doppler image for the secondary (K0) of V824 Ara is shown in Fig. 4. In this instance 9 independent spectral line profile were used in the reconstruction process. (Additional co-adding of the individual observations was done to improve the signal to noise in order to bring out the features in the weaker lines of the secondary.) These are shown as crosses in Fig. 5. The lines represent the fit provided by the Doppler image.

The image of the secondary also seems to be dominated by a polar spot (albeit smaller in area than its counterpart on V824 Ara B) whose center is also displaced from the rotation pole

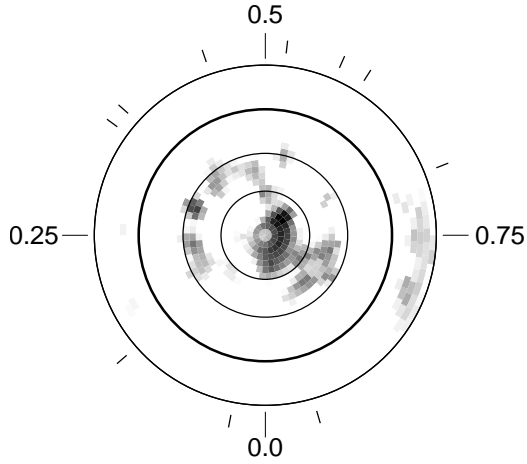


Fig. 4. Doppler image of V824 Ara B

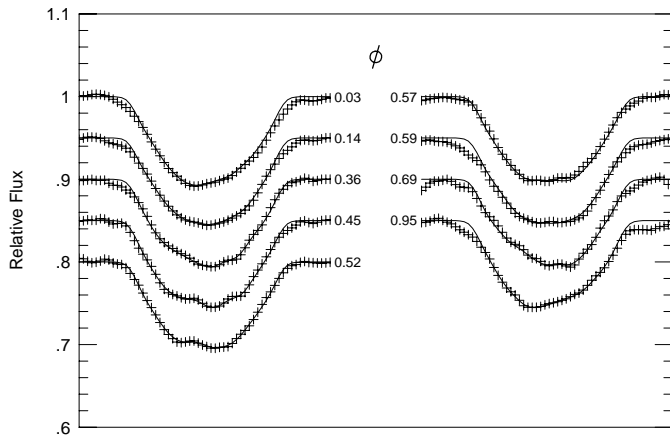


Fig. 5. The observed spectral line profiles of the Ca I 6439 Å line for V824 Ara B (crosses) and the fits from the Doppler image in Fig. 4

of the star. Again, there is also a series of small spots lying along latitude  $+30^\circ$  on the opposite side of the star in the phase range 0.2 to 0.5. The low-latitude features at phase 0.75 are most likely mirroring at negative latitudes of the feature near the visible pole. As shown by Vogt et al. (1987), weak “mirror” images of spot features in the “northern” hemisphere of the star can appear at opposite latitudes of the star.

The most striking feature about the Doppler images of the V824 Ara A/B is that they are very nearly mirror images of each other (i.e. the images look identical if one reverses or flips one with respect to the other). This is seen more clearly in Fig. 6 which shows the two Doppler images side by side. The radii and relative separation of the stars are drawn to scale. In this instance the flattened polar representations are shown as a thresholded version down to the equator. All regions of the star (pixels) with temperatures more than 500 K below the temperature of the photosphere are displayed as black while all other pixels are displayed as white. This version of the Doppler image shows only the major, more robust features of the spot distribution. The mirroring of the spot distribution is also evident in the spectral line profiles. The spectral line profiles of each star look nearly

identical (particularly at phase 0.03 and 0.95) when reversing spectral profiles of one star with respect to those of the other.

#### 4. Photometry

Photometric measurements for V824 Ara were made by Cutispoto & Leto (1997) in 1990 September. These are shown as solid circles in Fig. 7. We used our Doppler image of both components of V824 Ara to produce three different predicted light curves that was compared with this photometry. The first used the thresholded Doppler images shown in Fig. 6. This fit is shown as a solid line in Fig. 7. The dotted line in Fig. 7 shows the predicted light curve with the mid-latitude spots present. The fact that these features are rather small may be an indication that they are artifacts of mirroring (as explained in Sect. 3.3). Finally, the dashed line in Fig. 6 shows the predicted light curve generated by assuming only the polar spot on the primary (unspotted secondary).

Although all synthetic light curves produce the overall shape of the observed photometry (a minimum near phase 0.2 and a maximum near phase 0.80) they all fail to fit the observed amplitude. The best fit is provided by assuming that the secondary component is unspotted. This assumption is clearly unreasonable given the distortions that are obviously present in the spectral line of the secondary. The next best solution is provided by assuming that the high-latitude polar spots are the only true features of the Doppler image. A probable explanation for this discrepancy comes from the fact that the photometry was taken almost two months prior to the time of Doppler images, so it may not be valid to compare the predicted light curve to the measured one. Changes in the spot distribution between the times of the two data sets may well account for the discrepancy between the predicted and measured light curve. The only conclusion one may draw is that the minimum in the observed light curve that occurs near orbital phase 0.2 is most likely due to the high latitude spot on the primary which is facing the observer at this phase.

#### 5. Discussion

The Doppler images for V824 Ara A/B resemble more the Doppler images of young, pre-main sequence stars such as V410 Tau (Strassmeier et al. 1994; Joncour et al. 1994; Hatzes 1995) and HDE 283572 (Joncour et al. 1995). Both these young stars show large polar spots whose center is displaced from the rotation axis of the star. In contrast, RS CVn-type stars show large, centered polar spots often with large appendages extending down to low-latitudes. It seems that the Doppler images for V824 Ara A/B are consistent with the system being a pre-main sequence binary with an evolutionary age typical for weak T Tauri stars, although more Doppler images need to be derived for young stars before one can make reliable morphological comparisons between the spot distributions of evolved RS CVn-type stars and younger stars.

One drawback of the Doppler imaging technique is that it is virtually impossible to reconstruct reliably features that appear

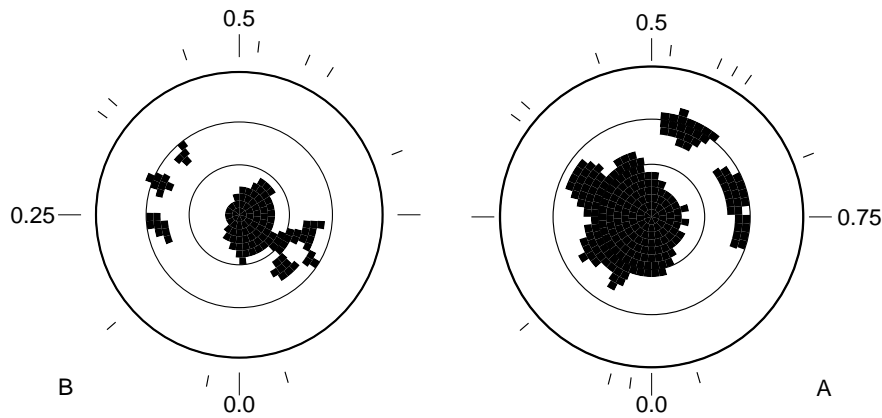


**Fig. 6.** The V824 Ara system. The stellar radii and separations are to scale.

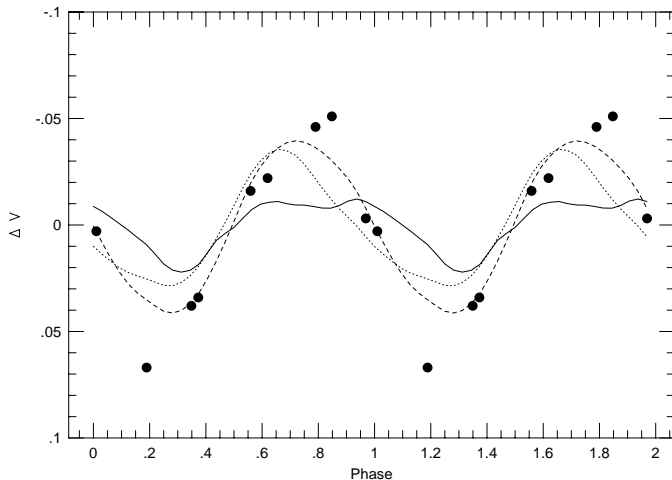


**Fig. 7.** (solid circles): The *V*-band light curve for V824 Ara taken by Cutispoto in 1990 September. (solid line): The predicted light curve using the thresholded Doppler images (Fig. 6). (dotted line): The predicted light curve from the thresholded images without the mid-latitude spots. (dashed line): The predicted light curve assuming only the primary is spotted.

at the most negative latitudes (near the hidden rotation pole); such features will always be reconstructed at higher latitudes. The mid-latitude spots seen on V824 Ara A/B may well be an artifact of such mirroring. One intriguing possibility is that these mid-latitude spots represent mirroring of a decentered spot at the opposite pole of the star, or possibly extensions or appendages of such a “southern” polar spot. Perhaps the two polar caps mark the location of a global dipole field whose axis is inclined with respect to the rotation axis of the star. Such oblique dipole fields are required by some star formation theories in order to explain the bipolar outflows (Shu et al. 1994).

With only one Doppler image it is difficult to assess the significance of the polar spot centers on both stars being displaced toward the direction of the companion. If additional Doppler

images establish that the decentering of the polar spot is always in this direction then this would imply that somehow the polar spots on each star knows of the presence of the companion. The fact that the spot distributions of V824 Ara A and B appear as mirror images of each other seems to suggest that tidal forces may play an important role in dictating the spot distribution on these stars. Clearly V824 Ara is a very important star for future Doppler imaging studies on the effects of stellar binarity on the spot distribution of active stars.

*Acknowledgements.* APH acknowledges the support of NSF grant AST-9315115 and AST-0615571.

## References

- Cutispoto G., Leto G., 1997, *A&AS* 121, 369  
 Donati J.-F., Collier Cameron A., 1997, *MNRAS* 291, 1  
 Hatzes A.P., 1995, *ApJ* 451, 784  
 Hatzes A.P., Penrod G.D., Vogt S.S., 1989, 341, 456  
 Herbst W., 1989, *AJ* 98, 2268  
 Joncour I., Bertout C., Menard F., 1994, *A&A* 285, L25  
 Joncour I., Bertout C., Bouvier J., 1995, *A&A* 291, L19  
 Kürster M., 1993, *A&A* 274, 851  
 Kürster M., Hatzes A.P., Pallavicini R., Randich S., 1992, In: Giampapa M., Bookbinder J. (eds.) *Proceedings 7th Cambridge Workshop on Cool Stars, Stellar systems and the Sun*. ASP Conf. Ser. Vol. 26, p. 249  
 Kürster M., Schmitt J.H.M.M., Cutispoto G., 1994, *A&A* 289, 899  
 Martin E.L., Brandner W., 1995, *A&A* 294, 744  
 Pasquini L., Cutispoto G., Gratton R., Mayor M., 1991, *A&A* 248, 72  
 Stout-Batalha N.M., Vogt S.S., 1996, In: Strassmeier K.G., Linsky J.L. (eds.) *IAU Symposium 176, Stellar Surface Structure*. p. 337  
 Strassmeier K.G., Welty A.D., Rice J.B., 1994, *A&A* 285, L17  
 Shu F.H., Najita J., Ostriker E., et al., 1994, *ApJ* 429, 781  
 Unruh Y.C., Cameron. A.C., Cutispoto G., 1995, *MNRAS*, 227, 1145  
 Valenti J.A., Piskunov N., 1996, *A&AS* 118, 595  
 Vogt S.S., Penrod G.D., Hatzes A.P., 1987, *ApJ* 321, 496  
 Walter F.M., Cash W., Charles P.A., Boyer C.S., 1980, *ApJ* 236, 212